Copepod secondary production in the sea: errors due to uneven molting and growth patterns and incidence of carcasses

Sonia Yáñez[1,2], Pamela Hidalgo[2], Paula Ruz[2,3], Kam W. Tang[4]

1. Doctoral Program in Oceanography, Department of Oceanography, Faculty of Natural Science and Oceanography, University of Concepcion, P.O. Box 160 C, Concepción, Chile

2. Department of Oceanography and Millennium Institute of Oceanography, Faculty of Natural Science and Oceanography, University of Concepcion, P.O. Box 160 C, Concepción, Chile.

3. Escuela de Ciencias del Mar, Pontificia Universidad Católica de Valparaíso, Valparaiso, Chile

4. Department of Biosciences, Swansea University, Swansea, SA2 8PP, U.K.

Corresponding author: P. Hidalgo (pahidalg@udec.cl)

Abstract

Secondary production of copepods is one of the basic parameters that govern the structure and function of the marine pelagic food web, and it is commonly estimated as cumulative biomass increase through consecutive molting based on short-term molting rate (MR) incubation experiments. The accuracy of the method depends on two underlying assumptions: (1) Even stage duration and inter-molt growth; (2) All copepods *in situ* are alive. We conducted a year-long study in a coastal bay within the Humboldt Current System to assess the errors in copepod secondary production estimation when these assumptions are violated. Abundances of live and dead individuals of the dominant species: *Paracalanus* cf. *indicus*, *Acartia tonsa* and *Calanus chilensis* were measured monthly. Concurrent molting rate experiments were conducted to derive copepod secondary production. A modified MR formulation was used to correct the secondary production estimates for error in assumption (1), and the live/dead copepod data were used to correct the estimates for error in assumption (2). Violation of the underlying assumptions caused error in secondary production estimation, most severely in *P.* cf. *indicus*. The error was not evenly distributed across the months, and in the case of *C. chilensis*, it switched between over- and under-estimation repeatedly. The annual average error was -39.2% in *P.* cf. *indicus*, 3.1% in *A. tonsa*, and 5.2% in *C. chilensis*. The errors also varied in magnitude and in sign among developmental stages, with some stages yielding nearly 70% over-estimation. For copepod species with short generation times, even small errors could quickly propagate and result in highly skewed secondary production projection. Reliable secondary production measurements therefore require careful assessment of species-specific stage duration and between-stage growth when applying the MR method, and quantification of stage-specific live and dead individuals in the field.

Keywords: Secondary production, copepods, non-predatory mortality, carcasses, molting rate method, coastal upwelling

1. Introduction

The population dynamics of copepods—the dominant metazoan zooplankton—is governed by three fundamental processes: Reproduction, growth, and mortality. Of these, reproduction is the most frequently measured as egg production by adult copepods (Mauchline, 1998). Somatic growth of adult copepods is often assumed to be negligible, whereas growth of younger stages can be challenging to measure, and in the absence of relevant data, it is often (incorrectly) assumed to be equal to adult reproduction rate (Hirst and Bunker, 2003). As the younger stages develop, they molt and increase somatic mass between stages. This characteristic allows scientists to conduct short-term incubation experiments and measure molting and biomass change between consecutive stages, from which they derive the growth rate—this is the commonly used molting rate (MR) method for estimating copepod secondary production (Runge et al., 1985; Kimmerer and McKinnon., 1987). Theoretical study and meta-analysis of literature data, however, suggest that the MR method is subject to errors when researchers fail to account for uneven stage duration and uneven somatic growth between stages (Hirst et al., 2005, 2014). Nevertheless, direct evaluation of errors associated with the MR method in the field has not been attempted.

The final parameter, mortality, is perhaps the least constrained in copepod population dynamics (Runge et al., 2004). Traditional research for convenience assumes that mortality is driven solely by predation and therefore can be derived from changes in population abundances. A corollary to this practice is that field sampling simply ignores the live/dead status of the animals. It is, however, illogical to believe all copepods *in situ* are alive. Copepods and other zooplankton can suffer non-predation mortality that leaves behind carcasses (Tang et al., 2014). A meta-analysis of literature data suggests that up to one-third of *in situ* copepod mortality cannot be explained by predation (Hirst

and Kiørboe, 2002). Ignorance of carcass occurrences also causes errors to other population parameters because dead copepods obviously do not molt, grow or reproduce. A modelling study showed that ignoring even a small magnitude of carcass abundance and non-predation mortality could lead to unrealistic projection of population growth (Elliott and Tang, 2011).

Here we report a year-long field study where we measured and compared the secondary production of different copepod species, and assessed the errors due to uneven molting and growth patterns and occurrence of carcasses. Our results showed that error in secondary production estimation varied among co-existing species, and switched between over-and under-estimation according to months or developmental stages. Reliable secondary production measurements therefore require careful assessment of species-specific stage duration, between-stage growth and stage-specific live/dead composition in the field, especially for species with a short generation time.

2. Materials and Methods

2.1 *in situ* live/dead copepod compositions

The study was conducted in northern Chile (Mejillones Bay) within the Humboldt Current System (HCS). This region is known for its active and intermittent coastal upwelling (Marín et al., 1993) that brings in shallow, oxygen-poor cold water masses associated with the Oxygen Minimum Zone (OMZ) (Marín and Olivares, 1999), and supports high levels of primary production (Daneri et al., 2000) and fish yield (Alheit and Bernal, 1993; Arcos et al., 2001).

Its metazooplankton community is dominated by copepods (Hidalgo et al., 2010; Escribano et al., 2012; Pino-Pinuer et al., 2014). Monthly sampling was performed in 2010 at three stations along a coastal transect: St–1 (23º 04.2’S, 70º 25.8’W; maximum

112 station depth (z_{max}) = 60 m), St–2 (23º 02.4'S, 70º 27.0'W; z_{max} = 90 m) and St–3 (23º
113 0.2'S, 70º 28.2'W; z_{max} = 120 m). Water temperature, salinity, and dissolved oxygen
114 (DO) were measured at each station by an autonomous profiler SeaBird SBE–19. Water
115 samples were collected at 10 m (within the mixed layer) using a 5-L Niskin bottle, and
116 their chlorophyll-*a* contents were analyzed fluorometrically (Morales and Anabalon,
117 2012; Anabalon et al., 2014).
118 Copepods were collected by vertical hauls through 0–30 m during the day using a
119 WP–2 net with a non-filtering cod (200 µm mesh and 50-cm mouth diameter) equipped
120 with a flowmeter. Our target copepod species are concentrated in this upper layer and
121 do not exhibit diel vertical migration in this region (Escribano et al., 2009). Upon
122 retrieval of the net, the samples were transferred to a chilled thermal box and
123 immediately treated with the vital stain Neutral Red (Elliott and Tang, 2009; modified
124 by Yanez, 2009 and Yanez et al., 2012 for local conditions). Briefly, each sample was
125 incubated with 2 – 4 mL of Neutral Red stock solution (0.5% w/v) for 10 min.
126 Afterward, the stained samples were concentrated and briefly rinsed with filtered
127 seawater to remove excess stain, then preserved in 4% neutralized formalin solution in
128 the dark, and processed further in the laboratory within 3 – 6 months. In the laboratory,
129 the stained samples were concentrated and briefly rinsed with filtered seawater, then
130 acidified by 0.3 mL of 1M acetic acid to develop the stain's color. Under a stereo-
131 microscope (20 – 40 X), the dominant copepod species *Paracalanus* cf. *indicus*, *Acartia*
132 *tonsa* and *Calanus chilensis* were counted and identified to developmental stages.
133 Individuals there were alive at the time of sampling appeared red, whereas dead ones
134 remained unstained.
135

136 **2.2 Molting rate experiments**

Molting rate experiments were conducted with the three dominant copepod species in the region: *P.* cf. *indicus*, *A. tonsa*, and *C. chilensis*. Copepods were collected by oblique tows of a WP–2 net with a non–filtering cod end from the upper 50 m at St–2 and St–3. The samples were immediately diluted in seawater and transported to the laboratory within 1 – 2 h. Additionally, seawater was collected with Niskin bottles at 10 m for the incubation. Upon return to the laboratory, live copepods were sorted by stage. Thirty individuals of each copepodid stage were randomly selected to measure prosome length, mean dry mass, carbon and nitrogen contents.

To determine mass–at–entry and mass–at–exit of each stage, stage C4, C5 and adult male and adult female individuals were each incubated in 23 µm-filtered seawater in 500 mL containers. A total of 45 individuals of C4, 40 C5, 80 adult male and 80 adult female were incubated at 15°C for 24h. Afterward, the animals were checked for stage and condition; those that had molted to the next stage were measured for prosome length, dry mass, carbon and nitrogen contents.

To set up the molting rate experiments, copepods were sorted in a temperature-controlled room set at near *in situ* temperature at 10-m depth. Groups of 10 individuals for each copepodid stage, in triplicate, were incubated in 200 mL vials containing 23-µm filtered seawater. Every 24 h, the initial stage, subsequent stage, molts and carcasses were counted. Dry masses of C1 and C2 were calculated from body lengths based on published conversion factors (Chisholm and Roff, 1990 for *P.* cf. *indicus* and *A. tonsa*; Escribano, 1998 for *C. chilensis*). For C3, C4 and C5 stages, dry masses were measured on a Cahn C-32 microbalance (0.001 mg precision) after being dried at 60°C for 24 h; body C and N contents were measured with a Thermo Scientific Flash EA 1112 HT Elemental Analyzer at the Universidad de Concepcion. We present all masses as geometric means for the specific stages. In total, we conducted 29 experiments with *P.*

cf. *indicus* in February, March, and April; 42 experiments with *A. tonsa* in February, April, August, September, and November, and 31 experiments with *C. chilensis* in August and September.

2.2 *In situ* copepod live/dead abundances

The mesh size we used was not appropriate for capturing the small nauplii; therefore, we only presented the data for copepodid stages (C1 to adult). To account for possible under-sampling of the small copepodid stages with the 200 µm mesh, we derived correction factors by comparing the abundances of all stages of each species caught by a 200 µm mesh vs. a 100 µm mesh (see equations (1) and (2) in Table 1; also Supplementary Material). Additionally, abundances were examined with a sensitivity analysis to assess their effect on the estimates of secondary production. The model responds accurately despite variation in the correction factor (between low and high values), suggesting it is a robust model (Figure S1 in Supplementary Material). Then we applied the correction factors only for C1-C3 of *Acartia tonsa* and *Paracalanus* cf. *indicus*, and C1 and C2 of *Calanus chilensis*, as there were no differences between mesh sizes for the later stages (Table S1 and Table S2 in Supplementary Material).

2.3 Secondary production calculations

Secondary productions of the three copepod species were calculated in different ways (Table 1). Firstly, we used the conventional MR equations to calculate the stage-specific secondary production, and the summation of all stages in each month gave the monthly secondary production for each species (NSP_{MR}). Next, we used the modified MR equations of Hirst et al., (2005) to calculate the monthly secondary production (NSP_H) by accounting for uneven stage duration and uneven between-stage growth.

Lastly, we corrected both secondary production estimates by accounting for the occurrence of carcasses (CSP_{MR} and CSP_{H}).

2.4 Statistics

Normality was tested by the Kolmogorov-Smirnov test (Zar, 1984). When necessary, the data were log transformed (n+1) to meet the requirement of normal distribution. Spatial (by stations) and temporal (by months) differences in the abundances of live and dead copepods were compared by ANOSIM pairwise comparisons. Seasonal growth rates (all stages combined) were grouped into Spring/Summer season (September–March) and Autumn/Winter season (April–August), and were then compared by t-test. Stage-specific growth rates (all months combined) were compared by ANOVA followed by Tukey's post–hoc test.

3. Results

3.1 General oceanographic conditions

The water column was thermally stratified except between July and September (Fig. 1a). The depth-average temperature ranged from 12.5 to 13.5 °C. Slightly less saline water masses were present in the upper 40 m for parts of the year (Fig. 1b). The depth-average salinity was 34.7–34.8 across the three stations. Well-oxygenated water was mostly limited to the upper 20 m (Fig. 1c). The upper limit of the OMZ (defined by DO = 1 mL O_2 L^{-1}) was at *ca.* 20 m during most of the year, except in August and November when it descended to ≥ 40m, coinciding with the weakening of thermal stratification and intrusion of less saline waters. Chlorophyll-*a* concentrations within the mixed layer were considerably higher in the austral summer/autumn months than in the winter/spring months, opposite to the DO trend (Fig. 2).

3.2 *In situ* copepod live/dead abundances

There were significant spatial, but not temporal, differences in live copepod abundances of *P.* cf. *indicus*, and the opposite for *A. tonsa* and *C. chilensis* (Table 2). The abundances of live copepods were generally higher closer to shore (St–1 and St–2) than offshore (St–3). Copepod carcasses were present throughout the year for all three species, and at times were comparable or even exceeding live copepod abundances (Fig. 3, 4 and 5). Contrary to live individuals, carcass abundances varied significantly between months, but not between stations for *P.* cf. *indicus*, and the opposite for *A. tonsa* and *C.chilensis* (Table 2). Carcasses of *P.* cf. *indicus* were dominated by the younger copepodites (C1– C3), and their percentages peaked in April and July/August. *A. tonsa* carcasses showed peak percentages in April and August, and were dominated by older stages (C4 – adult). In contrast, *C. chilensis* carcasses showed peak percentages in June and October, consisting of mostly C1 – C4, and a smaller November peak of adult carcasses.

3.3 Copepod molting and growth experiments

The stage duration ranged between 2.1 and 16 d for the different copepodid stages (C1– C5) of *P.* cf. *indicus*, whereas it was 1.2 – 10 d for *A. tonsa*, and 1.2 – 8 d for *C. chilensis*. None of the copepod species showed significant seasonal differences in growth rates ($P > 0.05$) (Table 3). Stage-specific growth rates of *P.* cf. *indicus*, *A. tonsa* and *C. chilensis* ranged from 0.15 – 0.23 d^{-1}, 0.14 – 0.20 d^{-1} and 0.10 – 0.27 d^{-1}, respectively (Table 3). Only *C. chilensis* showed significant variations in stage-specific growth rates ($P = 0.008$), caused by the significantly higher growth rate in C4 (Table 3).

236 **3.4 Secondary production estimations**

237 The estimated secondary production (sum of all stages; averaged across the three
238 stations) of *P.* cf. *indicus* showed the highest value in February and the lowest value in
239 September (Fig 6a). The production of *A. tonsa* had its highest value in March and
240 lowest in July, whereas the production of *C. chilensis* was concentrated in the autumn-
241 winter period (May – August) (Fig 6 b, c). The modified MR method produced
242 substantially different secondary production values for *P.* cf. *indicus* (6a), and the CSP_H
243 values were 33 – 96% higher than CSP_{MR}. In contrast, the CSP_H values were
244 comparable to CSP_{MR} for *A. tonsa* (within 1 – 13%) and *C. chilensis* (within 1 – 20 %;
245 Fig. 6 b, c).

246 Presence of carcasses introduced relatively small errors to the conventional MR
247 method (CSP_{MR} vs. NSP_{MR}) and lowered the estimation by an average of 2.3% (*P.* cf.
248 *indicus*), 0.8% (*A. tonsa*) and 2.6% (*C. chilensis*) (data not shown). Likewise, presence
249 of carcasses led to an average of 0.7 – 3.7% discrepancy between CSP_H and NSP_H (data
250 not shown).

251 By considering CSP_H as the "true" secondary production values, we estimated the
252 error associated with conventional MR method as $[(NSP_{MR}\text{-}CSP_H)/CSP_H]\times100\%$ (Table
253 4). The error was negative (i.e. underestimation) for *P.* cf. *indicus* throughout the year,
254 with a mean of 39.2% (SD 6.6%). The error was small and consistently positive for *A.*
255 *tonsa* (mean ± SD; 3.1 ± 2.8%). In contrast, the error switched sign repeatedly for *C.*
256 *chilensis*, and was concentrated in January, July and November (mean ± SD; 5.2 ±
257 14.9%) (Table 4).

258 Similarly, we calculated the stage-specific production and examined how the error
259 was distributed among the different stages (Fig. 7 a,b,c). For *P.* cf. *indicus*, most of the
260 error was associated with C1, C5 (*ca.* +65%) and C4 (-56%). For *A. tonsa*, the error was

concentrated in C4 and C5 (+61 to +69%). The largest error for *C. chilensis* was found in C2 (+66%), followed by C3 (+48%) and C4 (-38%).

4. Discussion

The HCS, as a part of the larger upwelling system off the west coast of South America, is a well–known, highly productive area for sardines and anchovies, which in turn support many predatory fish and bird species (Thiel et al., 2007). As both sardines and anchovies rely on zooplankton for food (Espinoza and Bertrand, 2008); much research effort has been dedicated to measuring the compositions, abundances, growth and production rates of the zooplankton, including copepods, within the HCS.

The water column of Mejillones Bay was characterized by thermal stratification and low DO for much of the year, except in winter months when the water column was more well mixed and the OMZ was restricted to the deeper depths, and when chlorophyll-*a* was nearly depleted. Previous studies have shown that changes in upwelling intensity (Escribano et al., 2012), the presence of thermal fronts, upwelling shadows acting as retention areas (Marín et al., 1993; Giraldo et al., 2002), and a shallow OMZ could aggregate and increase copepod diversity in the food–rich photic zone (Hidalgo and Escribano, 2008; Hidalgo et al., 2010). These factors, in addition to seasonal changes in food concentrations, affect the growth and development of copepods (Escribano, 1998; Poulet et al., 2007), and may explain the high temporal and spatial variabilities in copepod abundances in this study.

In past studies, copepod growth rates were estimated by fitting dry weight data to an exponential growth model (Escribano et al., 1997); alternatively, the MR method was used to resolve stage-specific growth rates (Vargas et al., 2007). The so–estimated growth rates were then applied to *in situ* biomass data to derive secondary production

(Escribano and McLaren, 1999; Vargas et al., 2007). These and other approaches, however, suffer a fundamental oversight by ignoring the *in situ* live/dead status of the copepods. It remains a common practice in field sampling where scientists simply preserve and count all copepods as 'live' (Harris et al., 2000). This has been partly due to the lack of methods for identifying live and dead individuals in the samples, and partly due to the ingrained perception that copepods only die of predation in the field (Hirst and Kiørboe, 2002). Recent advances in staining methods for distinguishing between live and dead individuals in field samples open the opportunities to make detailed quantification of copepod carcasses in the HCS, as well as to access the error they introduce into the secondary production estimation.

The total abundances of the three copepod species were higher closer to shore, similar to earlier observations (Escribano and Hidalgo, 2000; Giraldo et al., 2006). The abundances of both live and dead copepods varied considerably across stations, months and stages, reflecting the highly dynamic and heterogeneous environments in the region (Escribano, 1998; Giraldo et al., 2002; Escribano et al., 2012). Elliott and Tang (Elliott and Tang, 2009, 2011) observed higher percentages of carcasses and higher non-predation mortality rates in nauplii than in the older stages. Although we did not include nauplii in this study, we also found that the high carcass percentages were principally composed of young copepodites, suggesting that the younger stages were more susceptible to environmental stresses in this dynamic region, one of which could be the low DO. Intermittent intrusion of oxygen-poor water associated with coastal upwelling is a common feature in the region (Marín et al., 1993), which could cause episodic hypoxia and copepod mortality, similar to other studies (Yañez et al., 2012; Elliott et al., 2010, 2013).

Copepod carcasses are not necessarily lost from the food web. Some of them can be eaten by planktivores (Elliott et al., 2010), or be incorporated into the microbial food web (Tang et al., 2009; Bickel and Tang, 2010), with the remainder contributing to the sinking flux (Sampei et al., 2009, 2012; Ivory et al., 2014). Nevertheless, a dead copepod obviously "behaves" very differently than a live copepod, and understanding the fate of the carcasses will improve our knowledge of how they influence the ecosystem. More importantly, because dead individuals do not contribute to population growth, appropriate corrections are required for secondary production estimation.

While the MR method has been widely used to estimate secondary production (Runge and Roff., 2000), it is not without flaw (Rey-Rassat et al., 2002; Hirst et al., 2005, 2014). In this study, we quantified the errors in secondary production caused by the negligence of uneven stage duration and uneven between-stage growth, and the failure to differentiate live vs. dead copepods. Overall, our calculated range of errors based on field data was comparable to that derived from literature meta-analysis (Hirst et al., 2005, 2014). More importantly, our results showed that both the extent and sign of the error varied among the co–existing copepod species, and it was an order of magnitude higher in *P.* cf. *indicus* than in *A. tonsa* and *C. chilensis* (Table 4). *P.* cf. *indicus* is highly abundant throughout the HCS and plays major roles in the region's ecology (Escribano et al., 2012, 2016; Pino-Pinuer et al., 2014). This species is more likely to contribute carcasses than the other species, providing their greater abundance and potentially higher mortality. *P.* cf. *indicus* may rapidly respond to environmental variations (e.g. increased growth and development rates), and thus increasing the non-predatory mortality, as we observed in this study with the presence of carcasses. Our findings suggest that the secondary production estimation of this species is particularly error-prone, and extra caution is required when considering the regional food web

dynamics and fisheries involving this species. The average errors for *A. tonsa* and *C. chilensis*, despite their lower values, are still important for consideration because even a small initial error, when propagating through generations, would result in a large error over time (Elliott and Tang, 2011). This is particularly important for copepod species with short generation times, such as those in the HCS (Hidalgo and Escribano, 2008; Escribano et al., 2014). Equally important is the observation that, within species, the error distribution was not uniform across months or across stages (Table 4, Fig. 6). Knowing when and where most of the error occurs may help scientists to design more appropriate sampling and modelling strategies to minimize bias.

The Southwest Pacific region is strongly influenced by El Nino Southern Oscillation (ENSO). It is expected that climate change will intensify upwelling within the HCS (Echevin et al., 2012), with corresponding changes in hydrography, water chemistry, species diversity, and phenology (Hays et al., 2005). The potential increase in coastal upwelling events could promote blooms of chained diatoms that adversely affect the food supply for copepods (Vargas et al., 2006; Poulet et al., 2007). Stronger upwelling may also increase the shoaling of the OMZ and intensify hypoxia-related stresses. These projected changes may all lead to increasing incidents of non-predation mortality among the copepods. In future studies, efforts should be made to differentiate and quantify live and dead copepods *in situ*, and apply the appropriate corrections when estimating secondary production.

5. Conclusion

Copepod secondary production is a key parameter in ecology linking primary production to fishery yield, but reliable measurement of it remains challenging. This study used the first detailed quantitative data set of copepod live/dead compositions

within the Chilean HCS, along with molting rate measurements, to evaluate errors associated with copepod secondary production estimation. We showed that 1) copepod carcasses were ubiquitous in the region; 2) without proper corrections for uneven molting and growth patterns and carcass occurrence, there could be substantial errors in secondary production estimation; and 3) the magnitude and sign of the errors varied among months, species, and life stages; 4) carcass presence resulted in a relatively small % error when compared to choice of models (MR vs H), but even small % error caused by the ignorance of live/dead composition may lead to a large error in production projection (Elliott and Tang, 2011), especially for species with a short generation time.

Acknowledgements

This work was supported by the CONICYT-FONDECYT No. 11090146 (P. Hidalgo) and CONICYT Collaborative Project CHILE–USA No. USA2012–0006 (P. Hidalgo). Yañez was supported by the Scholarship of CONICYT-PCHA/Doctorado Nacional/2013-21130213 and by Red Doctoral en Ciencia, Tecnología y Ambiente, REDOC CTA, University of Concepcion. Ruz was supported by the Scholarship of CONICYT-PCHA/Doctorado Nacional/2011-21110560. The authors thank Dr. David Elliott for helping with data analysis, Captain Juan Menares and the crew of R/V Menachos for assistance in the field, and Dr. Andrew Hirst and Prof. Thomas Kiørboe for valuable comments and suggestions on earlier drafts of the manuscript. This work is a contribution by Millennium Institute of Oceanography ICM 120019.

References

Alheit, J., Bernal, P., 1993. Effects of physical and biological changes on the biomass yield of the humboldt current ecosystem. In: Sherman, K., Alexander, L.M., Gold, B.D.

(Eds.), Large Marine Ecosystems. American Association for the Advancement of Science Press, Washington, DC, pp. 53–58.

Anabalón, V., Arísteguia, J., Morales, C.E., Andrade, I., Benavides, M., Correa-Ramírez, M. A., Espino, M., Ettahiri, O., Hormazabal, S., Makaoui, A., Montero, M.F., Orbi, A., 2014. The structure of planktonic communities under variable coastal upwelling conditions off Cape Ghir (31°N) in the Canary Current System (NW Africa). Progr. Oceanogr. 120, 320–339.

Arcos, D.F., Cubillos, L.A., Nuñez, S.P., 2001. The jack mackerel fishery and El Niño1997–98 effects of Chile. Progr. Oceanogr. 49, 597–617.

Bickel, S.L., Tang, K.W., 2010. Microbial decomposition of proteins and lipids in copepod versus rotifer carcasses. Mar. Biol. 157, 1613–1624.

Chisholm, L., Roff, J., 1990. Size-weight relationships and biomass of tropical neritic copepods off Kingston, Jamaica. Mar. Biol. 106, 71–77.

Daneri, G., Dellarossa, V., Quiñonez, R., Jacob, B., Montero, P., Ulloa, O., 2000. Primary production and community respiration in the Humboldt Current System off Chile and associated oceanic areas. Mar. Ecol. Prog. Ser. 97, 41–49.

Echevin, V., Goubanova, K., Belmadani, A., Dewitte, B., 2012. Sensitivity of the Humboldt Current system to global warming: a downscaling experiment of the IPSL-CM4 model. Climate Dynam. 38, 761–774.

Elliott, D.T., Tang, K.W., 2009. Simple staining method for differentiating live and dead marine zooplankton in field samples. Limnol. Oceanogr. Methods 7, 585–594.

Elliott, D.T., Harris, C.K., Tang, K.W., 2010. Dead in the water: The fate of copepod carcasses in the York River estuary, Virginia. Limnol. Oceanogr. 55, 1821-1834.

Elliott, D.T., Tang, K.W., 2011. Influence of carcass abundance on estimates of mortality and assessment of population dynamics in *Acartia tonsa*. Mar. Ecol. Prog. Ser. 427, 1–12.

Elliott, D.T., Pierson, J.J., Roman, M., 2013. Copepods and hypoxia in Chesapeake Bay: abundance, vertical position and non-predatory mortality. J. Plankton Res. 0, 1-8.

Escribano, R., Irribarren, C., Rodriguez, L., 1997. Influence of food quantity and temperature on development and growth of the marine copepod *Calanus chilensis* from northern Chile. Mar. Biol. 128, 281–288.

Escribano, R., 1998. Population dynamics of *Calanus chilensis* in the Chilean eastern boundary Humboldt Current. Fish. Oceanogr. 7, 241–251.

Escribano, R., McLaren, I., 1999. Production of *Calanus chilensis* in the upwelling area of Antofagasta, northern Chile. Mar. Ecol. Progr. Ser. 177, 147–156.

Escribano, R., Hidalgo, P., 2000. Spatial distribution of copepods in the north of the Humboldt Current region off Chile during coastal upwelling. J. Mar. Biol. Assoc. UK 80, 283–290

Escribano, R., Hidalgo, P., Krautz, C., 2009. Zooplankton associated with the oxygen minimum zone system in the northern upwelling region of Chile during March 2000. Deep-Sea Res. II 56, 1083–1094.

Escribano, R., Hidalgo, P., Fuentes, M., Donoso, K., 2012. Zooplankton time series in the coastal zone off Chile: Variation in upwelling and responses of the copepod community. Progr. Oceanogr. 97, 74–186.

Escribano, R., Hidalgo, P., Valdes, V., Frederick, L., 2014. Temperature effects on development and reproduction of copepods in the Humboldt Current: the advantage of rapid growth. J. Plankton Res. 36, 104–116.

Escribano, R., Bustos-Ríos, E., Hidalgo, P., Morales C.E., 2016. Non-limiting food conditions for growth and production of the copepod community in a highly productive upwelling zone. Cont. Shelf Res. 126, 17–14.

Espinoza, P., Bertrand, A., 2008. Revisiting Peruvian anchovy (*Engraulis ringens*) trophodynamics provides a new vision of the Humboldt Current system. Progr. Oceanogr. 79, 215–227.

Giraldo, A., Escribano, R., Marin, V.H., 2002. Spatial distribution of *Calanus chilensis* off Mejillones Peninsula (northern Chile): ecological consequences upon coastal upwelling. Mar. Ecol. Progr. Ser. 230, 225–234.

Giraldo, A., Escribano, R., Marin, V.H., 2006. A field test of temperature effects on ecophysiological responses of copepodid *Calanus chilensis* during coastal upwelling in northern Chile. Cont. Shelf Res. 26, 1307–1315.

Harris, R., Wiebe, P., Lenz, J., Skjoldal, H.R., Huntley, M., 2000. ICES Zooplankton Methology Manual. Academic Press. San Diego, USA.

Hays, G., Richardson, A., Robinson, C., 2005. Climate change and marine plankton. Trends Ecol. Evol. 20, 337–344.

Hidalgo, P., Escribano, R., 2008. The life cycles of two coexisting copepods, *Calanus chilensis* and *Centropages brachiatus*, in the upwelling zone off northern Chile (23ºS). Mar. Biol. 155, 429–442.

Hidalgo, P., Escribano, R., Vergara, O., Jorquera, E., Donoso, K., Mendoza, P., 2010. Patterns of copepod diversity in the Chilean coastal upwelling system. Deep-Sea Res. Part II 57, 2089–2097.

Hirst, A.G., Bunker, A.J., 2003. Growth of marine planktonic copepods: global rates and patterns in relation to chlorophyll a, temperature, and body weight. Limnol. Oceanogr. 48, 1988–2010.

457 Hirst, A. G., Kiørboe, T., 2002. Mortality of marine planktonic copepods: global rates
458 and patterns. Mar. Ecol. Progr. Ser. 230, 195–209.
459 Hirst, A.G., Peterson, W.T., Rothery, P., 2005. Errors in juvenile copepod growth rate
460 estimates are widespread: problems with the Moult Rate method. Mar. Ecol. Progr. Ser.
461 296, 263–279.
462 Hirst, A.G., Keister, J.E., Richardson, A.J., Ward, P., Shreeve, R.S., Escribano, R.,
463 2014. Re-assessing copepod growth using the Moult Rate Method. J. Plankton Res. 36,
464 1224–1232.
465 Ivory, J.A., Tang, K.W., Takahashi, K., 2014. Use of Neutral Red in short-term
466 sediment traps to distinguish between zooplankton swimmers and carcasses. Mar. Ecol.
467 Progr. Ser. 505, 107–117.
468 Kimmerer, W. J., McKinnon, D., 1987. Growth, mortality, and secondary production of
469 the copepod *Acartia tranteri* in Westernport Bay, Australia. Limnol. Oceanogr. 32, 14–
470 28.
471 Marín, V., Rodríguez, L., Vallejo, L., Fuenteseca, J., Oyarce, E., 1993. Efectos de la
472 surgencia costera sobre la productividad primaria primavera de la Bahía Mejillones de
473 Sur (Antofagasta, Chile). Rev. Chil. Hist. Nat. 66, 479–491.
474 Marín, V., Olivares, G., 1999. Estacionalidad de la productividad primaria en Bahía
475 Mejillones del Sur (Chile): una aproximación proceso-funcional. Rev. Chil. Hist. Nat.
476 72, 629–641.
477 Mauchline, J., 1998. The Biology of Calanoid Copepods. Advances in Marine Biology
478 vol. 33. Academic Press.
479 Morales, C.E., Anabalon, V., 2012. Spatio-temporal distribution of chlorophyll-a,
480 picoplankton, and nanoplankton during the spring upwelling season in the coastal area
481 off Concepción, central-southern Chile. Progr. Oceanogr. special volume.

Pino-Pinuer, P., Escribano, R., Hidalgo, P., Riquelme-Bugueño, R., Schneider, W., 2014. Copepod community response to variable upwelling conditions off central-southern Chile during 2002−2004 and 2010−2012. Mar. Ecol. Progr. Ser. 515, 83–95.

Poulet, S.A., Escribano, R., Hidalgo, P., Cueff, A., Wichardc, T., Aguilera, V., Vargas, C.A., Pohnert, G., 2007. Collapse of *Calanus chilensis* reproduction in a marine environment with high diatom concentration. J. Exp. Mar. Bio. Ecol. 352, 187–199.

Rey-Rassat, C., Irigoien, X., Harris, R., Head, R., Carlotti, F., 2002. Growth and development of *Calanus helgolandicus* reared in the laboratory. Mar. Ecol. Progr. Ser. 238, 125–138.

Runge, J.A., McLaren, I.A., Corkett, C. J., Koslow, J.A., 1985. Molting rates and cohort development of *Calanus finmarchicus* and *Calanus glacialis* in the sea southwest Nova Scotia. Mar. Biol. 86, 241–246.

Runge, J.A., Roff J.C., 2000. The measurement of growth and reproductive rates. In: Harris R (ed) ICES zooplankton methodology manual. Academic, New York, pp. 401–454.

Runge, J.A., Franks, P.J., Gentleman, W.C., Megrey, B.A., Rose, K.A., Werner, F.E., and Zakardjian, B., 2004. Diagnosis and prediction of variability in secondary production and fish recruitment processes: developments in physical-biological modelling. In: Robinson AR, Brink KH (eds) The sea, vol. 13. Harvard University Press, pp. 413–473.

Sampei, M., Sasaki, H., Hattori, H., Forest, A., Fortier, L., 2009. Significant contribution of passively sinking copepods to downward export flux in Arctic waters. Limnol. Oceanogr. 54, 1894–1900.

Sampei, M., Sasaki, H., Forest, A., Fortier, L., 2012. A substantial export flux of particulate organic carbon linked to sinking dead copepods during winter 2007-2008 in

the Amundsen Gulf (southeastern Beaufort Sea, Arctic Ocean). Limnol. Oceanogr. 57, 90–96.

Tang, K.W. Bickel, S.L. Dziallas, C. and Grossart, H.P. 2009. Microbial activities accompanying decomposition of cladoceran and copepod carcasses under different environmental conditions. Aquat. Microb. Ecol. 57, 89–100.

Tang, K.W., Gladyshev, M.I., Dubovskaya, O., Kirillin, G., Grossart H.P., 2014. Zooplankton carcasses and non-predatory mortality in freshwater and inland sea environments. J. Plankton Res. 36, 597–612.

Thiel M., 37 others. 2007. The Humboldt current system of northern and central Chile. Oceanography and Marine Biology: An Annu. Rev. 45, 195–344.

Vargas, C.A., Escribano, R., Poulet, S., 2006. Phytoplankton diversity determines time windows for successful zooplankton reproductive pulses. Ecol. 87, 2992–2999.

Vargas, C.A., Martínez, R.A., Cuevas, L.A., Pavez, M.A., Cartes, C., González, H.E., Escribano, R., Daneri, G., 2007. The relative importance of microbial and classical food webs in a highly productive coastal upwelling area. Limnol. Oceanogr. 52, 1495–1510.

Wetzel, R.G.. 1995. Death, detritus, and energy flow in aquatic ecosystems. Fresh. Biol. 33, 83-89.

Yáñez, S., 2009. Tasa de mortalidad y desarrollo de *Paracalanus cf. indicus* (Copepoda: Calanoida) (Wolfender, 1905) en la zona Centro-Sur de Chile (36°S) asociada con la zona de mínimo de oxígeno. Seminario de título, Facultad de Ciencias Naturales y Oceanográficas, Universidad de Concepción, Concepción, 65 pp.

Yañez, S., Hidalgo, P., Escribano, R., 2012. Mortalidad natural de *Paracalanus indicus* (Copepoda, Calanoida) en áreas de surgencia asociada a la zona de mínimo oxígeno en el Sistema de Corrientes de Humboldt: implicancias en el transporte pasivo del flujo de carbono. Rev. Biol. Mar. Oceanogr. 47, 295–310.

532 Zar, J.H., 1984. Biostatistical Analysis. Prentice-Hall International Inc., New Jersey,
533 718 pp.

534

535

536 Table 1. Parameters and formulations for calculating copepod secondary production.

Parameter	Symbol	Unit	Note
Molting rate	MR	d^{-1}	Stage-specific MR is indicated by subscript *i*
Number of individuals in molting rate experiment	N		Consecutive stages are indicated by subscripts *i* and *i+1*
Time	T	h	
Mean weight of stage *i*	W_i	mg	
Mean weight of stage *i+1*	W_{i+1}	mg	
Total biomass *in situ*	B_i	mg C m^{-2}	No differentiation of live and dead individuals
Biomass of live individuals *in situ*	B_{i_a}	mg C m^{-2}	
Numerical abundance *in situ*	n_i	m^{-2}	No differentiation of live and dead individuals
Numerical abundance of live individuals *in situ*	n_{i_a}	m^{-2}	
Abundances Correction Factor	CFn_i	no unit	Abundances of dead individuals
Abundances Correction Factor	CFn_{i_a}	no unit	Abundances of live individuals
Stage-specific growth rate estimated from MR method	g_{i_MR}	d^{-1}	
Non-corrected secondary production from MR method	NSP_{MR}	mg C m^{-2} d^{-1}	No differentiation of live and dead individuals
Corrected secondary production from MR method	CSP_{MR}	mg C m^{-2} d^{-1}	NSP_{MR} estimates corrected for occurrence of carcasses
Proportion of animals which molted during incubation	M		Stage-specific M is indicated by the subscript *i*
Incubation period	L	d	
Stage duration	D	d^{-1}	Calculated as D = 1/MR
Mortality rates during incubation	B	d^{-1}	Calculated from proportion of carcasses according to Elliott and Tang (2011); stage specific β is indicated by subscript *i*
Actual development time of stage *i*	D_{i_actual}	d^{-1}	Calculated from stage-specific β_i and M_i
Actual development time of stage *i+1*	D_{i+1_actual}	d^{-1}	Calculated from stage-specific β_{i+1}, and M_{i+1}
Geometric mean weight of stage *i*	$\hat{W}_i$	mg	Including the weight of molt lost between stages
Geometric mean weight of stage *i+1*	$\hat{W}_{i+1}$	mg	Including the weight of molt lost between stages
Growth rate g_i from the mid-point of stages *i* to *i+1*	$g_{i\rightarrow i+1}$	d^{-1}	For C1-C4 stages
Growth rate g_i calculated based on W_{i_entry} and W_{i_exit}	g_{i_corr}	d^{-1}	For C5 where the following stage (*i+1*) does not molt (Hirst et al. 2005)
Mass at entry	W_{i_entry}	mg	Arithmetic mean weights at

			point of entry to C5
Mass at exit	W_{i_exit}	mg	Arithmetic mean weights at point of exit from C5
Non-corrected secondary production from modified MR method	NSP_H	mg C m^{-2} d^{-1}	No differentiation of live and dead individuals
Corrected secondary production from modified MR method	CSP_H	mg C m^{-2} d^{-1}	NSP_H estimates corrected for the occurrence of carcasses

Calculations of correction factor:

$$CF_i = \frac{n_{i(100\mu m)}}{n_{i(200\mu m)}} \quad (1)$$

$$CF_{i\_a} = \frac{n_{i\_a(100\mu m)}}{n_{i\_a(200\mu m)}} \quad (2)$$

Calculations of secondary production:

MR method (NSP_{MR}) (Runge et al. 1985; Kimmerer & McKinnon 1987)

$$MR = \left(\frac{N_i + N_{i+1}}{N_i}\right) \times t \quad (3)$$

$$g_{i\_MR} = \ln\left(\frac{W_{i+1}}{W_i}\right) \times MR_i \quad (4)$$

$$B_i = \sum_{i=1}^{N} (W_i\, n_i) \times 0.4 \quad (5)$$

Where 0.4 is the factor to convert dry weight to carbon (Escribano et al. 2007, 2016).

$$NSP_{MR} = \sum_{i=1}^{N} (B_i\, g_{i\_MR}) \quad (6)$$

MR method corrected for carcasses (CSP_{MR}). To correct NSP_{MR} for the occurrence of carcasses, equations (3) and (4) are changed to:

$$B_{i\_a} = \sum_{i=1}^{N} (W_i\, n_{i\_a}) \times 0.4 \quad (7)$$

$$CSP_{MR} = \sum_{i=1}^{N} (B_{i\_a}\, g_{i\_MR}) \quad (8)$$

Modified MR method (NSP_H) (Hirst et al. 2005)

$$M = \exp(-\beta D)[\exp(\beta L) - 1]/[1 - \exp(-\beta D)] \quad (9)$$

$$D_{i\_actual} = \ln\{1 + [\exp(\beta_i L) - 1]/M_i\}/\beta_i \quad (10)$$

$$g_{i \to i+1} = \ln\left(\frac{\hat{W}_{i+1}}{\hat{W}_i}\right) \div [(D_{i\_actual} + D_{i+1\_actual})/2] \quad (11)$$

$$g_{i\_corr} = \ln\left(\frac{W_{i\_exit}}{W_i}\right) \times MR_i \quad (12)$$

$$B_i = \sum_{i=1}^{N} (W_i\, n_i) \times 0.4 \quad (13)$$

$NSP_H = \sum_{i=1}^{N} (B_i \, g_i)$	(14)
Modified MR method corrected for carcasses (CSP_H). To correct NSP_H for the occurrence of carcasses, equations (11) and (12) are changed to:	
$B_{i\_a} = \sum_{i=1}^{N} (W_i \, n_{i\_a}) \times 0.4$	(15)
$CSP_H = \sum_{i=1}^{N} (B_{i\_a} \, g_i)$	(16)

537

538

539 Table 2: ANOSIM pairwise comparisons of abundances of live and dead individuals of
540 *Paracalanus* cf. *indicus*, *Acartia tonsa* and *Calanus chilensis* at different stations and
541 months in the Mejillones Bay during 2010. *r* value is the strength of the factors on the
542 samples (number of levels in each factor as stations=3, Months=12; * indicates
543 significant difference at $p < 0.05$.

Source of variance		*P.*cf. *indicus*		*A.tonsa*		*C.chilensis*	
		Live	Dead	Live	Dead	Live	Dead
Stations	*r*	0.643	-0.029	0.047	-0.059	0.002	-0.015
	p	0.001*	0.828	0.143	0.057	0.410	0.634
Months	*r*	-0.155	0.328	218	0.244	0.357	0.480
	p	0.960	0.001*	0.006*	0.011*	0.010*	0.010*

544
545
546

547 Table 3: Summary of seasonal and stage-specific growth rates (g; d^{-1}) (mean ± SD) of
548 *Paracalanus* cf. *indicus*, *Acartia tonsa* and *Calanus chilensis*. (n = number of
549 measurements).

	P. cf. *indicus*		*A. tonsa*		*C. chilensis*	
Spring/Summer	0.21 ± 0.07	(n = 140)	0.12 ± 0.06	(n = 60)	0.21 ± 0.05	(n = 60)
Autumn/Winter	0.20 ± 0.07	(n = 150)	0.18 ± 0.10	(n = 260)	0.21 ± 0.08	(n = 250)
C1	0.22 ± 0.02	(n = 30)	0.20 ± 0.01	(n = 30)	0.22 ± 0.08	(n = 50)
C2	0.19 ± 0.06	(n = 30)	0.16 ± 0.03	(n = 30)	0.10 ± 0.05	(n = 40)
C3	0.21 ± 0.07	(n = 100)	0.14 ± 0.03	(n = 60)	0.18 ± 0.05	(n = 50)
C4	0.23 ± 0.06	(n = 60)	0.15 ± 0.06	(n = 180)	0.27 ± 0.07	(n = 70)
C5	0.15 ± 0.01	(n = 70)	0.17 ± 0.04	(n = 120)	0.19 ± 0.06	(n = 100)

550

551

552 Table 4. Errors in secondary production estimates. By considering CSP_H as the "true"
553 secondary production values, we estimated the error associated with conventional MR
554 method as $[(NSP_{MR}-CSP_H)/CSP_H]\times100\%$. Negative and positive values represent the
555 underestimated and overestimated secondary production, respectively.

	Paracalanus cf. *indicus*	*Acartia tonsa*	*Calanus chilensis*
January	-46.3	1.2	14.9
February	-31.6	1.7	-0.5
March	-34.9	1.5	6.2
April	-22.6	6,2	-4.4
May	-37.0	4.0	-3.6
June	-43.8	1.2	6.6
July	-43.0	1.1	16.9
August	-42.1	0.8	-5.4
September	-27.9	2.8	-5.5
October	-35.7	1.9	-7.8
November	-50.4	5.1	45.2
December	-43.1	10.1	0.1
Mean	**-39.2**	**3.1**	**5.2**
S.D.	**6.6**	**2.8**	**14.9**

556

557

558 **Figure captions**

559 Figure 1: Oceanographic conditions off Mejillones Bay, northern Chile, in 2010
560 (average of three stations): (a) Temperature, (b) Salinity and (c) Dissolved oxygen.

561 Figure 2: Chlorophyll-*a* (at 10 m) and average DO (0–30 m) at St–1, St–2 and St–3 in
562 different months during this study.

563 Figure 3: Abundances of live and dead copepodid stage C1, C2, C3, C4, C5, and adults
564 (Ad) of *Paracalanus* cf. *indicus* at the three stations in different months.

565 Figure 4: Abundances of live and dead copepodid stage C1, C2, C3, C4, C5, and adults
566 (Ad) of *Acartia tonsa* at the three stations in different months.

567 Figure 5: Abundances of live and dead copepodid stage C1, C2, C3, C4, C5, and adults
568 (Ad) of *Calanus chilensis* at the three stations in different months.

569 Figure 6: Secondary production estimates and stage-specific errors for *Paracalanus* cf.
570 *indicus* (a), *Acartia tonsa* (b), and *Calanus chilensis* (c). CSP_{MR} is secondary production
571 estimates (sum of all stages; averaged across stations) based on conventional MR
572 method after correction for carcasses. CSP_H is secondary productions based on modified
573 MR method after correction for carcasses.

574 Figure 7: Stage-specific errors for *Paracalanus* cf. *indicus* (a), *Acartia tonsa* (b), and
575 *Calanus chilensis* (c) in secondary production estimation calculated based on average
576 (n=12) stage-specific NSP_{MR} and CSP_H (see text for explanation).

577

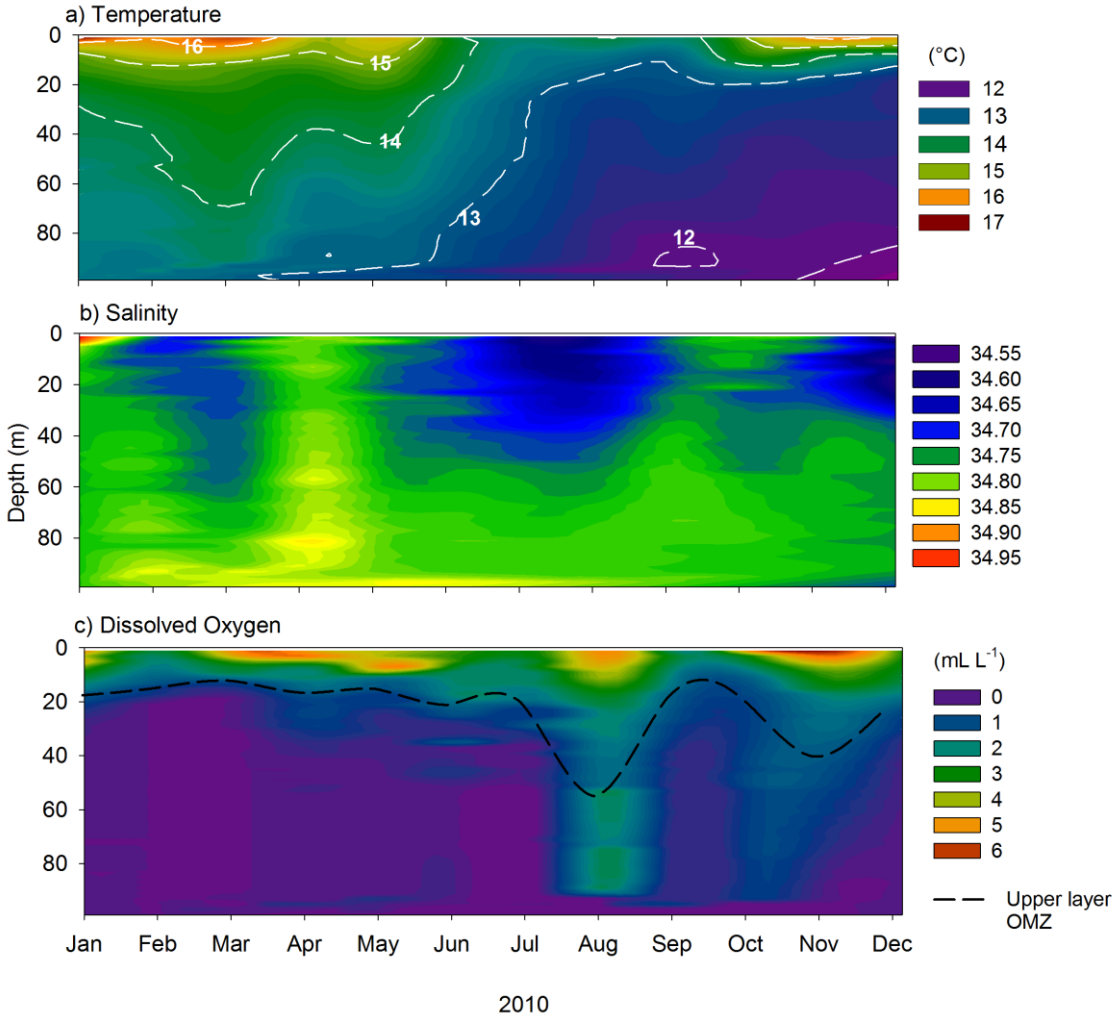

578
579 **Figure 1**

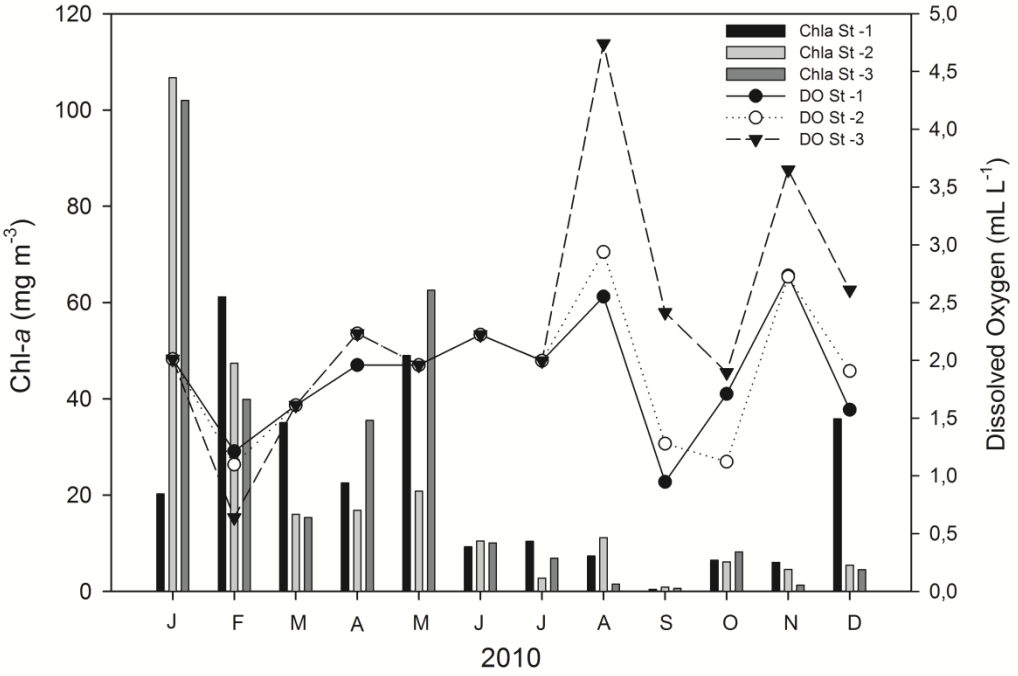

580
581 **Figure 2**

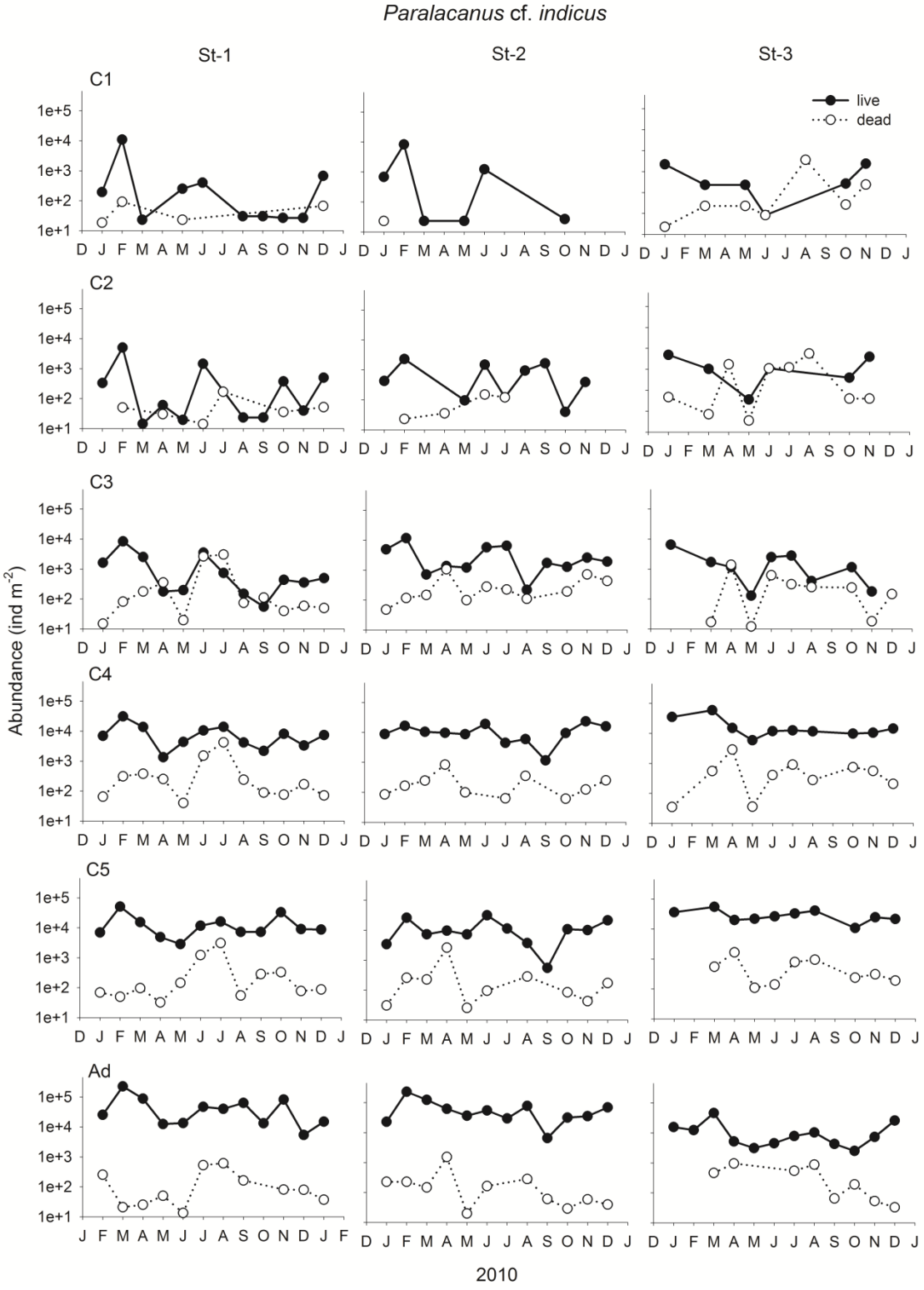

582
583 **Figure 3**

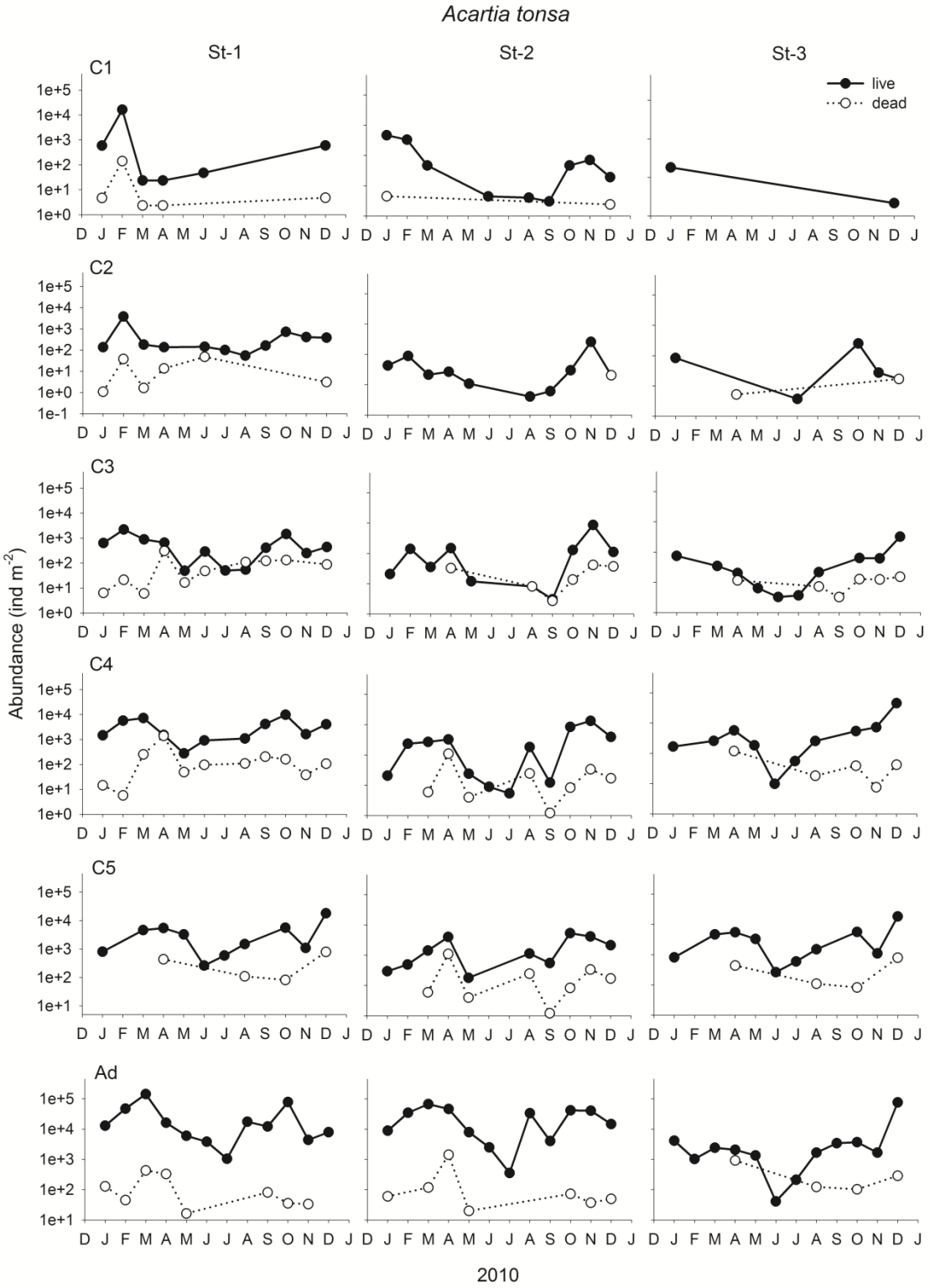

584
585 **Figure 4**

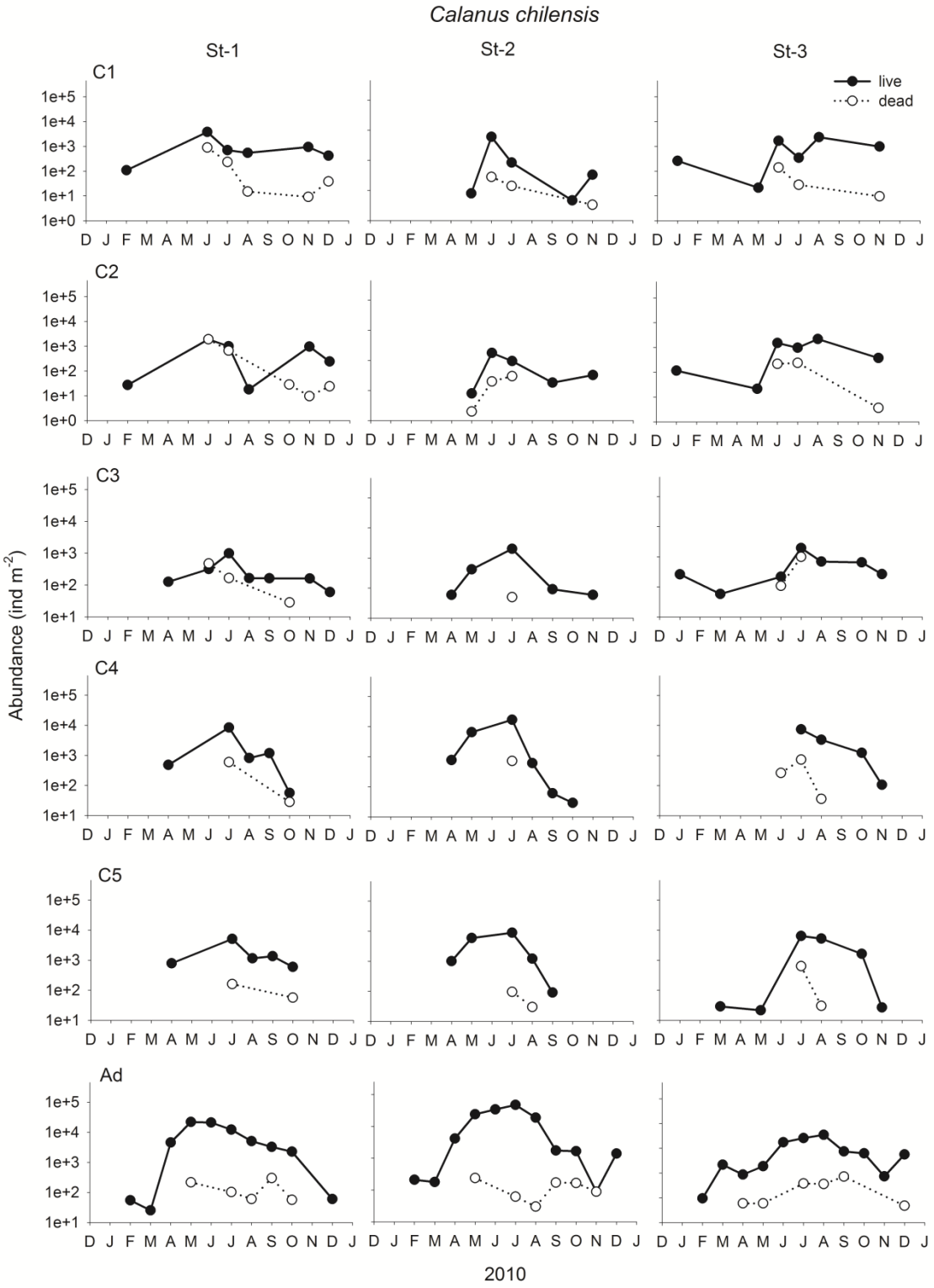

586
587 **Figure 5**

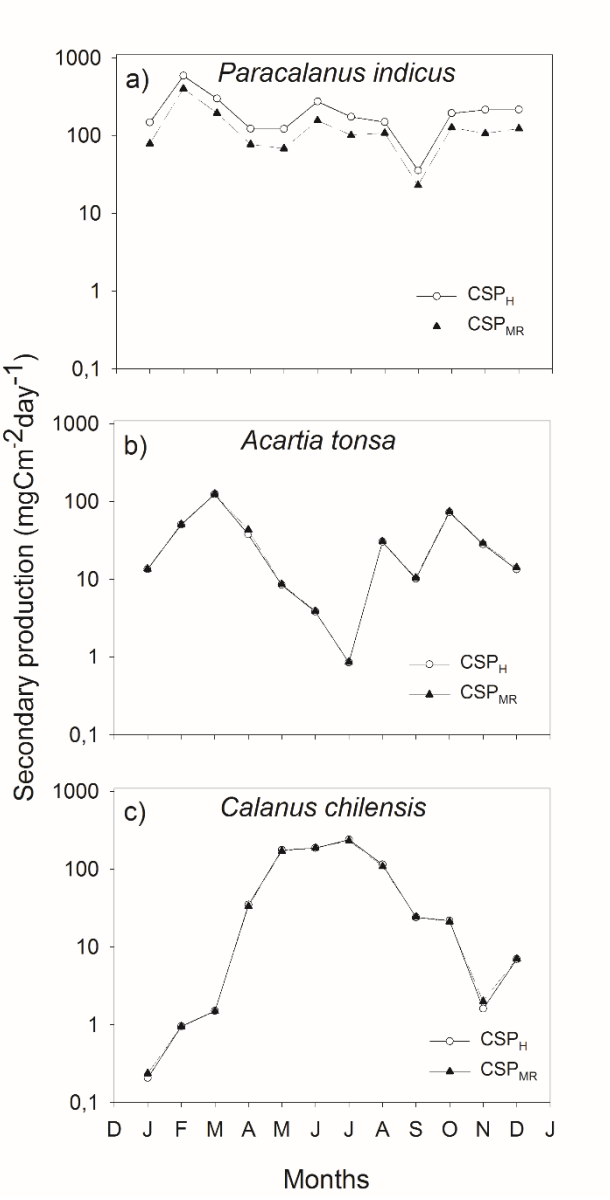

588

589 **Figure 6**

590

591

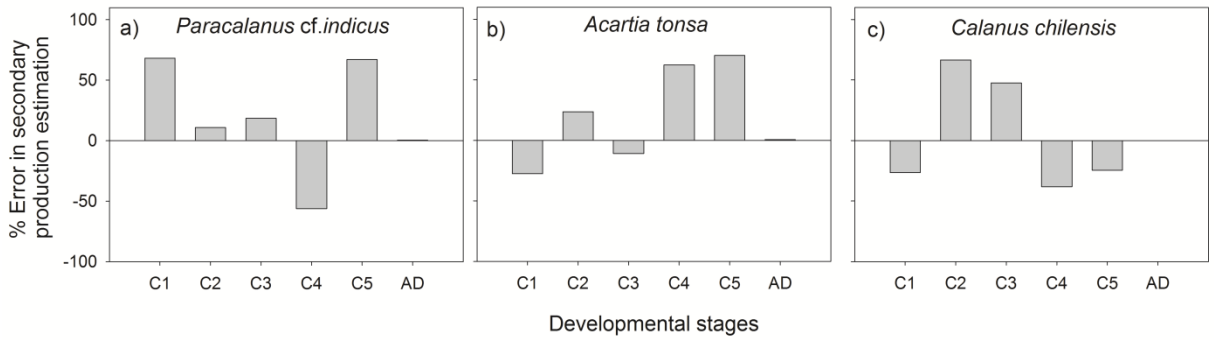

592

593 **Figure 7**

594

595